https://dx.doi.org/10.22161/ijaers.4.9.9 ISSN: 2349-6495(P) | 2456-1908(O)

Experimental Research on Performances of Air Turbines for a Fixed Oscillating Water Column-Type Wave Energy Converter

Tengen Murakami[1], Yasutaka Imai[1], Shuichi Nagata[1], Manabu Takao[2], Toshiaki Setoguchi[1]

[1]Institue of Ocean Energy, Saga University, Japan
[2]Department of Mechanical Engineering, National Institute of Technology, Matsue College, Japan

Abstract*—A fixed oscillating water column (OWC)-type wave energy converter is composed of an air chamber for primary conversion and an air turbine for secondary conversion. In the optimal design method of a fixed OWC-type wave energy converter, it is necessary to develop a design method which can consider the characteristics of incident wave motion, the motion of the internal free surface affected in the structure such as a partly submerged wall, the fluctuation of air pressure in an air chamber, the rotation of the air turbine. In this paper, the 2-dimensional wave tank tests in regular waves for the performance evaluation of the air turbines in a fixed OWC-type wave energy converter were conducted to obtain the data needed to make this design method. As the results, the effects of the impulse turbine specification such as the rotor inlet/outlet angle, the guide vane's number and the vane's setting angle on the primary and secondary conversion efficiencies are clarified experimentally. Furthermore, the performances of the Wells turbines with different number of blade are presented for comparison of the operating condition.*

***Keywords*— Wave energy converter, Oscillating water column, Primary and secondary conversion efficiencies, Impulse turbine, Wells turbine.**

I. INTRODUCTION

As for renewable energy resources in the world, we can newly exploit the mini-/micro-hydro, the wind, the solar and the ocean energy, etc. Wave energy which is one of the renewable energies attracts attention as a promising resource that can reduce CO_2 emissions. Wave energy converter (WEC) which converts wave power into electric power has been developed all over the world and many types of WECs [1] such as the movable body type [2,3] and the overtopping wave type [4] were proposed.

There is an oscillating water column (OWC)-type wave energy converter as one of the WECs. This device is composed of an air chamber, an air turbine and a generator and is expected to be safe even under storm conditions. Many studies on this device have been performed experimentally and theoretically since the early 1970s.

In the performance evaluation of the OWC-type WEC, it is necessary to consider the characteristics of the incident wave motion, the motion of the internal free surface affected in the structure such as a partly submerged wall, the fluctuation of air pressure in an air chamber, and the rotation of the air turbine. However, most of the past studies were carried out by dividing into two steps of the primary conversion and the secondary conversion.

To estimate the primary conversion performance, the many researches [5,6] on the air chamber with the nozzle as the substitute of the turbine were conducted. Wilbert et al. [7] carried out the wave flume tests to evaluate the hydrodynamic performance of Double Chamber Oscillating Water Column (DCOWC). Ning et al. [8] investigated the hydrodynamic performance of a fixed OWC wave energy device under various wave conditions and geometric parameters in a wave flume. In this study, the power take-off was implemented through a nozzle situated on the roof of the chamber. Though, the effects of the turbine are unclear in the above studies.

As concerns the secondary conversion, by means of the test rig having a piston-cylinder to generate the oscillating air flow, the performance of the air turbine was evaluated in a series of studies. Setoguchi et al. [9,10] reviewed a variety of experimental results concerning the performances of the Wells turbine and the impulse turbine. Besides, Takao et al. [11] showed that the impulse turbine was superior to the Wells turbine in a wide flow rate range.

On the other hand, there are the studies about the performance of the OWC with the turbine [12], but the most studies make mention of the performance of the OWC with the Wells turbine. Besides, the influences of the turbine geometry on the primary conversion and secondary conversion performances were not clarified.

https://dx.doi.org/10.22161/ijaers.4.9.9 *ISSN: 2349-6495(P) | 2456-1908(O)*

This paper discusses the geometry effects of the impulse turbine on the primary and secondary conversion efficiencies in the fixed OWC-type WEC based on the experimental data needed to make this design method. Additionally, the performance of the Wells turbine is compared with the one of the impulse turbine.

II. EXPERIMENTAL APPARATUS

Fig. 1 shows the arrangement of the experimental devices in the 2-dimensional wave tank. This tank is 18.5 m long, 0.8 m wide and contains 0.8 m water depth. An absorbing wave generator was installed at the end of the tank and the model turbine was located at the other end of the tank. Four wave height gauges (TS-DWG) produced by TECHNO SERVICE Co., Ltd. were arranged to measure the amplitudes of the incident wave accurately [13]. The wave data is fed into the computer through the analog-to-digital converter (PCI-3165) from the Interface Corporation. The incident wave height was configured as high as possible in this wave tank, and the value was 0.1 m.

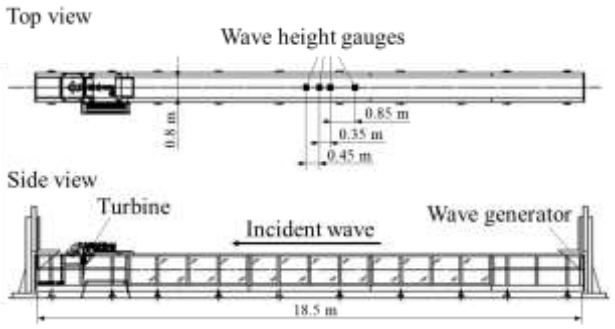

Fig. 1: Arrangements of model turbine and wave height gauges in 2-D wave tank

Fig. 2 shows the model of OWC-type wave energy converter with the impulse turbine. In the experiments, the turbine is rotated by the alternating-current synchronous motor (HG-JR73) manufactured by the Mitsubishi Electric Corporation. The torque transducer (SS-005) and the electromagnetic rotation detector (MP-981) produced by ONO SOKKI Co., Ltd. were located at the end of the turbine shaft. The air chamber length is 0.7 m, the curtain wall depth is 0.1 m and the thickness of the curtain wall is 0.005 m. The schematic design of the air chamber was conducted in a series of numerical studies [14].

Fig. 3 indicates the location of the pressure gauge (AP-10S) and the wave height gauges (FW-H07 and UD320) made by KEYENCE CORPORATION at the top of the air chamber. The rectangular orifice of the air chamber is located at the center. The data of waves, the turbine rotational speed, the torque, the pressure and the water surface elevation in the air chamber were measured simultaneously. The sampling frequency is 50 Hz and the data collection was started after the lapse of 30 seconds from the start of the wave generator.

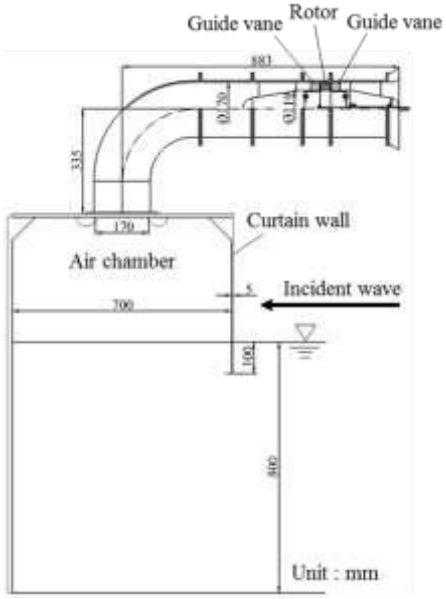

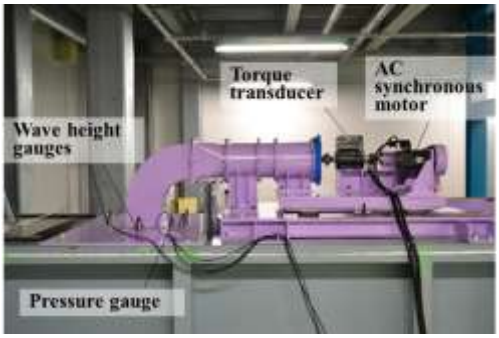

Fig. 2: Model OWC with impulse turbine

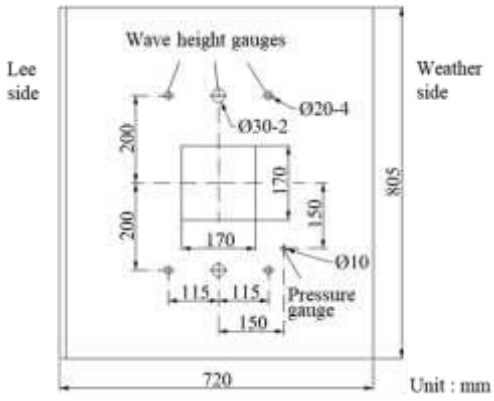

Fig. 3: Positions of pressure gauge and wave height gauges at top of air chamber

Fig. 4 shows the basic configuration of the rotor and the fixed guide vanes. This turbine configuration was adopted on the basis of the air turbine test results [9]. The numbers of the rotor blades and the single-stage guide vanes are 30

https://dx.doi.org/10.22161/ijaers.4.9.9 *ISSN: 2349-6495(P) | 2456-1908(O)*

and 26, respectively. The inlet/outlet angle γ of rotor is 60 degrees and the setting angle θ of guide vane is 30 degrees. The inner diameter D of turbine casing is 170 mm, the hub ratio ν is 0.7 and the clearance between the rotor blade tip and the casing is 0.3 mm. The inner diameter D of the turbine casing was determined based on the condition that the total pressure drop at the turbine is equal to the total pressure difference at the nozzle which the ratio of cross-section between the nozzle and the air chamber is 1/100.

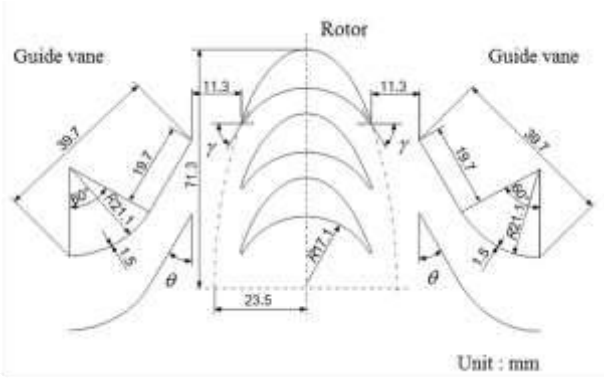

Fig. 4: Configuration of rotor and guide vane

Besides, we conducted the steady flow turbine test. In this test without waves, the bottom of the air chamber was closed by an acrylic board as shown in fig. 5 and the steady flow was generated by a centrifugal fan.

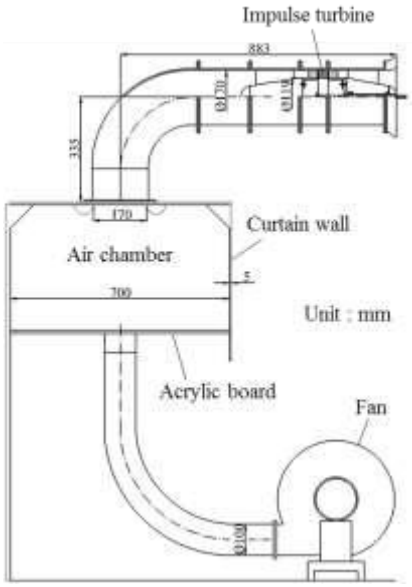

Fig. 5: Model for steady flow test

III. EXPERIMENTAL RESULTS

3.1 Impulse Turbine

3.1.1 Effect of number of guide vanes

Fig. 6 shows a comparison of the efficiencies between the three cases with different number Z_g of guide vanes. The abscissa is the ratio between the wave length λ and the air chamber length L. In this experiment, the wave length λ was changed while keeping the time-averaged rotational speed of turbine N = 700 rpm. The wave periods are T = 1.00 sec., 1.15 sec., 1.30 sec., 1.41 sec., 1.50 sec., 1.56 sec., 1.65 sec., 1.73 sec., 1.87 sec., 2.03 sec., 2.30 sec. and 2.63 sec. The primary conversion efficiency η_1, the secondary conversion efficiency η_2 and the generating efficiency η are defined as:

$$\eta_1 = \frac{P_{air}}{P_{wave}} \tag{1}$$

$$\eta_2 = \frac{P_{torque}}{P_{air}} \tag{2}$$

$$\eta = \frac{P_{torque}}{P_{wave}} \tag{3}$$

where P_{air} is the time-averaged power of the air, P_{wave} is the time-averaged power of the incident wave and P_{torque} is the turbine output. The definitions of these parameters are as follows:

$$P_{air} = \frac{S}{T}\int_0^T p(t)\frac{\partial \zeta}{\partial t}dt \tag{4}$$

$$P_{wave} = \frac{1}{2}\rho_w g \zeta_i^2 C_g W \tag{5}$$

$$P_{torque} = \frac{1}{T}\int_0^T T_0 \omega dt \tag{6}$$

where S, p, ζ, ρ_w, g, ζ_i, C_g, W, T_0 and ω denote the cross-section area of air chamber, the pressure, the six averaged water level in the air chamber, the water density, the gravitational acceleration, the incident wave amplitude, the group velocity, the chamber width, the turbine output torque and the angular velocity of turbine, respectively.

As shown in fig. 6, the maximum generating efficiency η is achieved at around λ/L = 6.3 in all three cases Z_g = 32, 26 and 20.

Next, the rotational speed N was changed while keeping the ratio λ/L = 6.3 as shown in fig. 7. The maximum generating efficiency η was achieved at about N = 700 rpm in all three cases Z_g = 32, 26 and 20. Meanwhile, the high generating efficiency of about 0.28 was obtained in two cases of Z_g = 32 and 26. On the other hand, the maximum value of η decreased in the case of Z_g = 20. The remarkable difference of η appeared at higher speed than 1000 rpm according to the η_2. It seems that the decrease of the η_2 was caused by the reduction of the whirl velocity of flow from the upstream guide vane based on the flow separation in the case of Z_g = 20.

https://dx.doi.org/10.22161/ijaers.4.9.9 *ISSN: 2349-6495(P) | 2456-1908(O)*

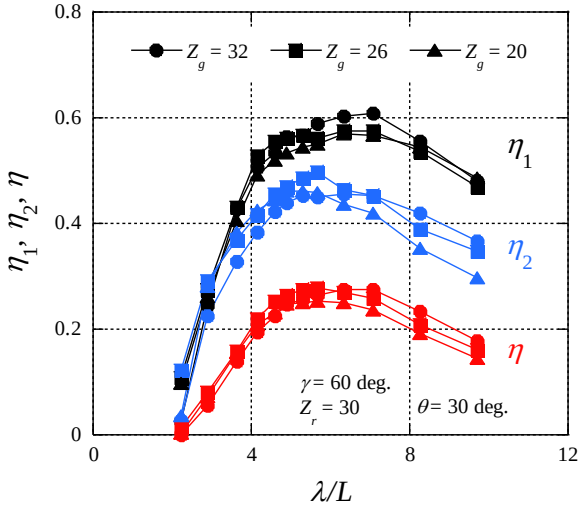

Fig. 6: Change in efficiencies due to number of guide vane at time-averaged rotational speed N = 700 rpm

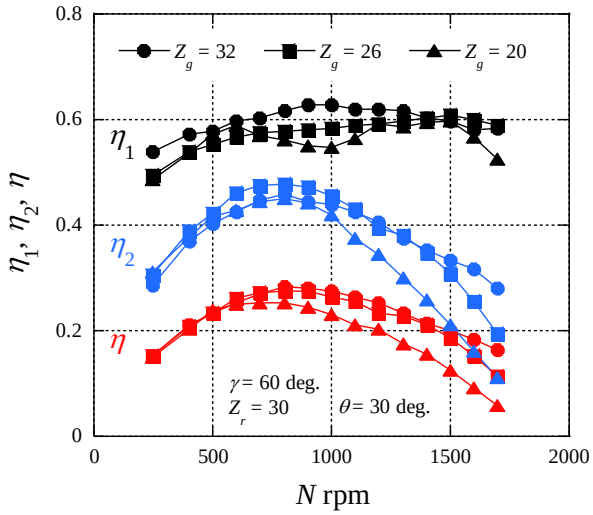

Fig. 7: Change in efficiencies due to number of guide vane at λ/L = 6.3

3.1.2 Effect of setting angle of guide vane

To know the effects of the setting angle θ of guide vane on the primary and secondary conversion efficiencies, the θ was varied from the base case of 30.0 degrees to 37.5 degrees and 22.5 degrees. In fig. 8, the efficiencies are compared between the above three cases. The number of guide vanes is Z_g = 26 giving the high efficiency. The ratio λ/L was kept constant at 6.3. As shown in fig. 8, the effect of the θ on the η_1 is small at about N = 700 rpm giving the maximum η. Besides, the maximum value of the η is highest at θ = 30.0 degrees.

Figs. 9 and 10 show the amplitudes of the pressure and the water surface elevation in the air chamber. It is found that the pressure increases at smaller θ. Meanwhile, the amplitude of the water surface elevation decreases inversely with the pressure rise. Therefore, the difference of the η_1 due to the θ is small in fig. 8.

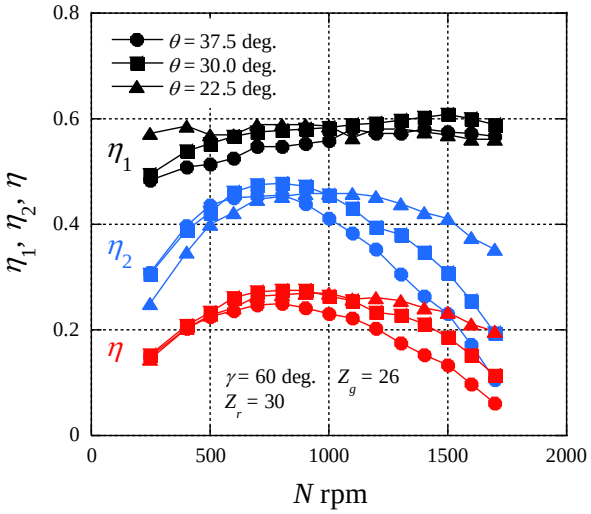

Fig. 8: Change in efficiencies due to setting angle of guide vane at λ/L = 6.3

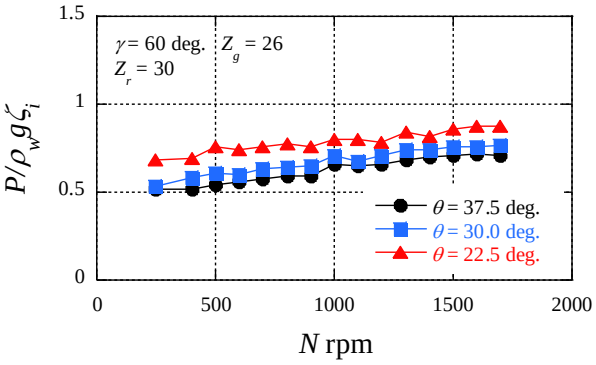

Fig. 9: Pressure amplitude in air chamber

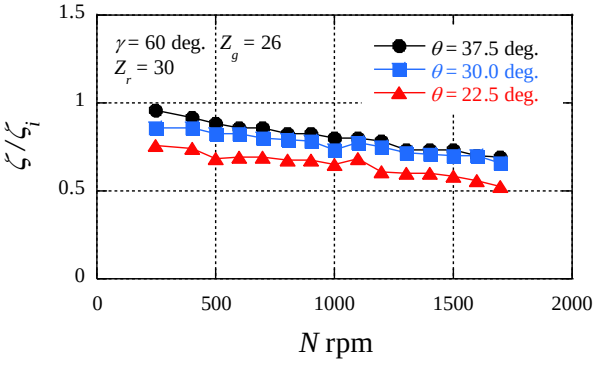

Fig. 10: Water surface elevation in air chamber

Fig. 11 shows the turbine performances in three cases of the above different θ in waves and the result of the steady flow test in fig. 5, where C_T is the torque coefficient, C_A is

https://dx.doi.org/10.22161/ijaers.4.9.9 *ISSN: 2349-6495(P) | 2456-1908(O)*

the input coefficient and the abscissa ϕ is the flow coefficient. The definitions of these parameters are as follows:

$$C_T = \frac{T_0}{\rho(v_a^2 + U^2)S_T r / 2} \quad (7)$$

$$C_A = \frac{\Delta p}{\rho(v_a^2 + U^2)/2} \quad (8)$$

$$\phi = \frac{v_a}{U} \quad (9)$$

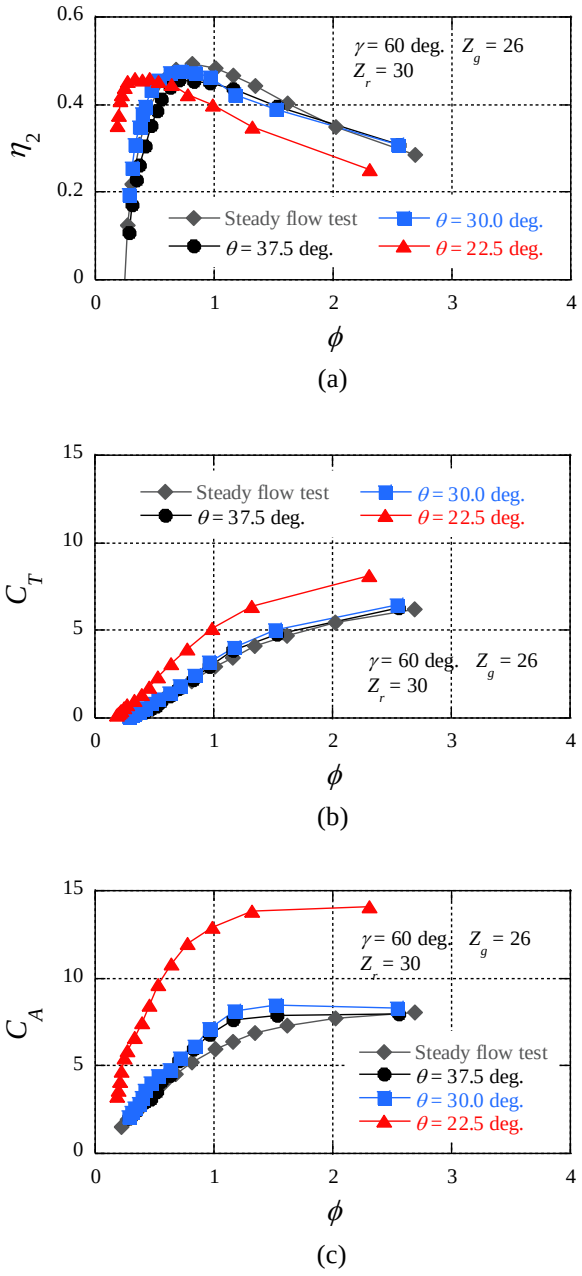

Fig. 11: Turbine performance: (a) secondary conversion efficiency, (b) torque coefficient and (c) input coefficient

where ρ, v_a, U, S_T and Δp are the air density, the axial velocity, the circumferential velocity at mean radius r [= $D(1+\nu)/4$], the flow passage area of turbine and the total pressure drop at the turbine. In the steady flow test, the inlet/outlet angle γ of rotor is 60 degrees, the number Z_g of guide vanes is 26 and the setting angle θ of guide vane is 30 degrees.

In fig. 11(a), the maximum η_2 of about 0.48 was obtained at ϕ = 0.71 in the case of θ = 30.0 degrees in wave test results, and the value is almost the same level as the case of the steady flow test. On the other hand, in both cases θ = 37.5 degrees and 22.5 degrees, the maximum η_2 decreased slightly. In addition, the flow coefficient giving the maximum η_2 became small by reduction of the θ from 30.0 degrees to 22.5 degrees. Furthermore, in the case of θ = 22.5 degrees, the C_A increased markedly at around ϕ = 0.45 of the maximum efficiency point compared with the other cases in fig. 11(c). This fact corresponds to the pressure rise in fig. 9. In the case of θ = 22.5 degrees, along with the pressure rise, the turbine output torque becomes higher at small flow rate due to the increase of the whirl velocity of flow from the upstream guide vane as shown in fig. 11(b). This is the reason why the peak of η_2 appeared in the small flow rate.

3.1.3 Effect of inlet/outlet angle of rotor

The inlet/outlet angle of rotor was changed from γ = 60 degrees to 50 degrees. Fig. 12 shows the variations of the efficiencies due to the rotational speed.

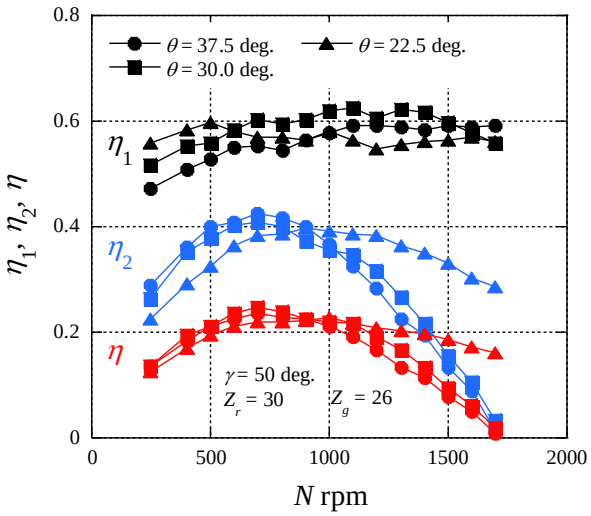

Fig. 12: Efficiencies at γ = 50 degrees

In addition, fig. 13 shows the secondary conversion efficiency as a function of the flow coefficient. The trend shifting the peak of η_2 to the small flow rate region at θ = 22.5 degrees in fig. 13 is similar to the one of the case of γ

https://dx.doi.org/10.22161/ijaers.4.9.9 *ISSN: 2349-6495(P) | 2456-1908(O)*

= 60 degrees in fig. 11(a), although the maximum value of η_2 decreased. This reduction of η_2 causes the deterioration of the η as shown in fig. 12.

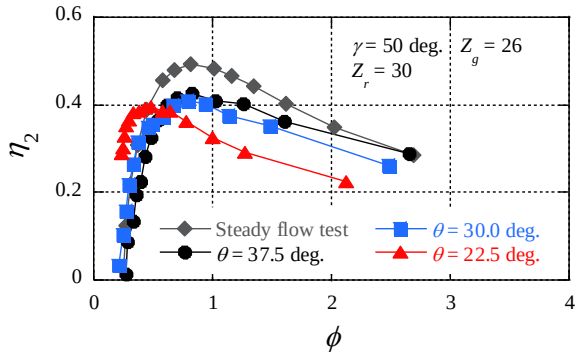

Fig. 13: Change in secondary conversion efficiency due to flow coefficient

Fig. 14 shows a comparison of the efficiency between three cases with different inlet/outlet angle γ of rotor. The setting angle θ of guide vane is 30 degrees. It is noticed that the effect of γ on the η_1 is small at about N = 700 rpm giving the maximum η, and the highest η_2 and η are achieved in the case γ = 60 degrees. As the above results, the recommended impulse turbine consists of the inlet/outlet angle γ = 60 degrees of rotor, the setting angle θ = 30 degrees of guide vane, the number Z_r = 30 of rotor blades and the number Z_g = 26 of guide vanes.

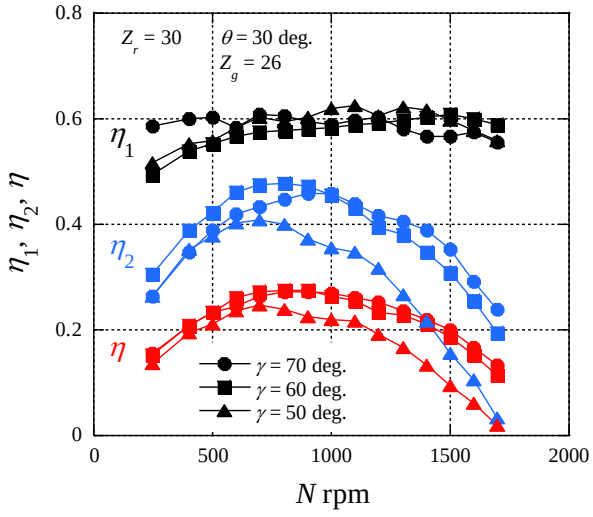

Fig. 14: Comparison of efficiency between three cases with different inlet/outlet angle of rotor

3.2 Wells Turbine

The energy conversion efficiency of the OWC model with the Wells turbine was measured for comparison with the one of the above impulse turbine. In fig. 15, the blades numbers of the Wells turbine without the guide vane are Z_r = 7, 6 and 5. In all three cases, the chord length is 51 mm, blade profile is NACA0020, the aspect ratio is 0.5 and the hub ratio is 0.7. In the case Z_r = 6, the solidity at mean radius is 0.67, and this value was adopted in the previous research on a performance in the steady flow condition [15].

Fig. 15: Wells turbine

Fig. 16 shows the efficiencies at λ/L = 6.3 in three cases Z_r = 7, 6 and 5. It is found that the operating speed range N of the Wells turbine is high compared with the one of the impulse turbine. And, it seems that the N giving the high η_2 and η shifts to the higher speed range with the decrease of the blade number, though the maximum η_2 and η are reduced in the case Z_r = 7. The maximum η_2 of about 0.48 and the maximum η of about 0.28 were achieved in both cases Z_r = 6 and 5. These maximum values are almost the same level as the ones of the impulse turbine in fig. 14.

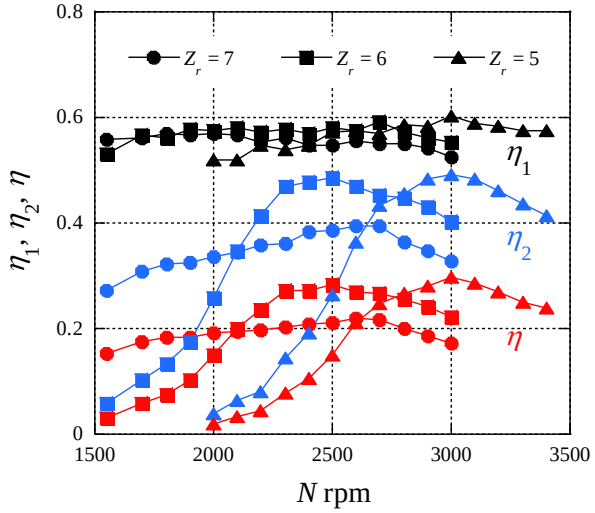

Fig. 16: Efficiencies in model OWC with Wells turbine

Figs. 17 and 18 are the amplitudes of the pressure and the water surface elevation in the air chamber. The pressure increased at the larger Z_r, and the amplitude of the water surface elevation decreased inversely with the pressure rise.

https://dx.doi.org/10.22161/ijaers.4.9.9 ISSN: 2349-6495(P) | 2456-1908(O)

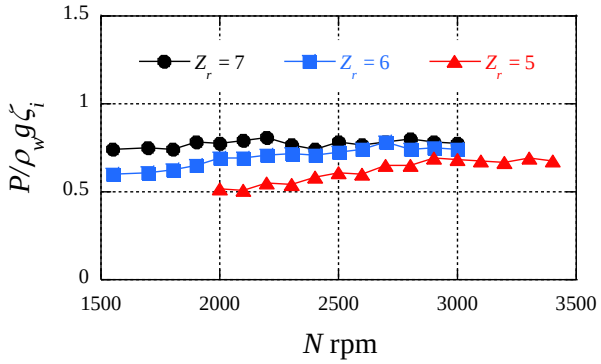

Fig. 17: Pressure amplitude

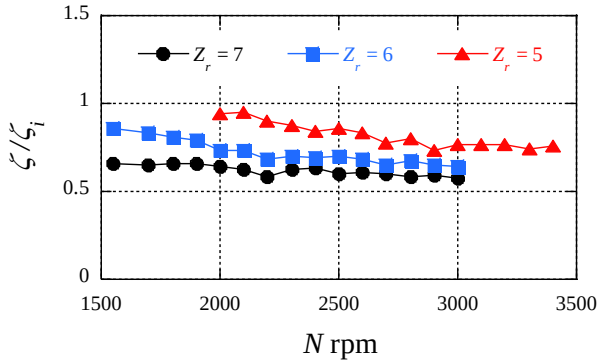

Fig. 18: Water surface elevation

Fig. 19 is a comparison of the turbine performances. The steady flow test results denote the performance of the impulse turbine in fig. 5 and the one of the Wells turbine having the casing diameter D = 300 mm in the previous research [15]. As shown in fig. 19, the maximum η_2 in all three cases Z_r = 7, 6 and 5 are obtained at about ϕ = 0.21, and the C_A increases with the pressure rise in fig. 17. In both cases Z_r = 6 and 5, the same high η_2 as the previous research on the steady flow performance of the Wells turbine is achieved. Meanwhile, the maximum η_2 becomes lower in the case Z_r = 7, because the increase of C_T corresponding to the increase of C_A is not sufficient. This is caused by the fact that the flow passage area at hub side is extremely narrow as shown in fig. 15.

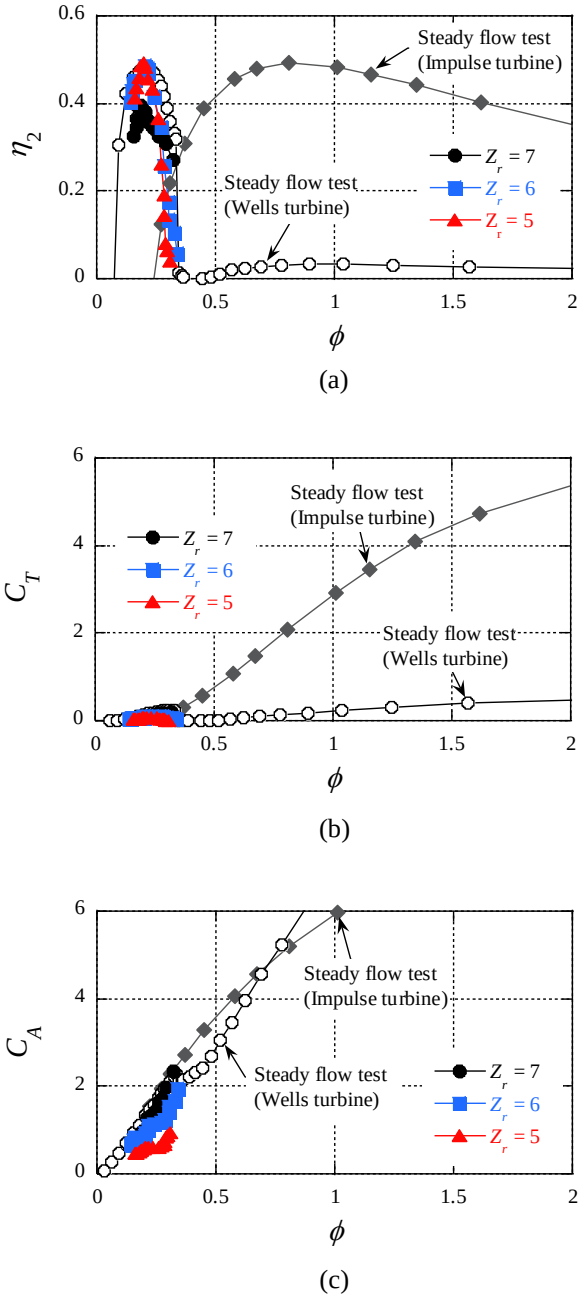

Fig. 19: Wells turbine performance: (a) secondary conversion efficiency, (b) torque coefficient and (c) input coefficient

IV. CONCLUSIONS

This paper discussed the effects of the impulse turbine specification such as the rotor inlet/outlet angle γ, the guide vane's setting angle θ and the guide vane's number Z_g on the primary conversion efficiency η_1, the secondary conversion efficiency η_2 and the generating efficiency η (= $\eta_1\eta_2$) in the fixed OWC-type WEC based on the results of the 2-dimensional wave tank tests.

In the experiments, the rotor inlet/outlet angle was changed between three cases γ = 70 degrees, 60 degrees and 50 degrees, and the guide vane's setting angle was varied from θ = 30.0 degrees to 37.5 degrees and 22.5 degrees. Besides, the single-stage guide vane's number was changed from Z_g = 26 to 32 and 20. Furthermore, the performances of the Wells turbines with different number Z_r of blades were investigated. The following concluding remarks are obtained.

1. The maximum generating efficiency of about 28% is

https://dx.doi.org/10.22161/ijaers.4.9.9 *ISSN: 2349-6495(P) | 2456-1908(O)*

achieved in both cases Z_g = 32 and 26.

2. In the case with γ = 60 degrees and θ = 30 degrees, the maximum secondary conversion efficiency of about 48% as high as the one in the steady flow condition is obtained.
3. The combination of γ = 60 degrees, θ = 30 degrees, Z_g = 26 and the rotor blade number Z_r = 30 is the promising specification of the impulse turbine.
4. As regards this experiment, the maximum secondary conversion efficiency in the OWC with the Wells turbine is almost the same level as the one of the impulse turbine.

ACKNOWLEDGEMENTS

This investigation was carried out under the "Program for the Promotion of New Energy Infrastructure Development", supported by the Mitsubishi Research Institute (MRI)/the Ministry of Economy, Trade and Industry (METI), Japan. It was also supported by a research grant of the Hatakeyama Culture Foundation.

REFERENCES

[1] Mehrangiz, S., Emami, Y., Sadigh, S. H. S., Etemadi, A. (2013). Various technologies for producing energy from Wave: a review, International Journal of Smart Grid and Clean Energy, vol.2, no.2, pp. 289–294.

[2] Watabe, T. (2008). Utilization of the ocean wave energy, Fuji Print Press.

[3] Cameron, L., Doherty, R., Henry, A., Doherty, K., Van't Hoff, J., Kaya, D., Naylor, D., Bourdier, S., Whittaker, T. (2010). Design of the next generation of the oyster wave energy converter, Proceedings of the 3rd International Conference on Ocean Energy, Spain, pp.1–12.

[4] Margheritini, L., Vicinanza, D., Frigaard, P. (2009). SSG wave energy converter: design, reliability and hydraulic performance of an innovative overtopping device, Renewable Energy, vol.34, pp.1371–1380.

[5] Takahashi, S., Ojima, R., Suzumura, S. (1985). Air power pneumatic-type wave power extractors due to irregular wave actions – a study on development of wave power, 3rd report, The Port Harbour Research Institute, vol.24, pp.3–41.

[6] Liu, Z., Hyun, B., Hong, K. (2008). Application of numerical wave tank to OWC air chamber for wave energy conversion, Proceedings of the Eighteenth International Offshore and Polar Engineering Conference, Canada, pp.350–356.

[7] Wilbert, R., Sundar, V., Sannasiraj, S. A. (2013). Wave interaction with a double chamber oscillating water column device, International Journal of Ocean and Climate Systems, vol.4, no.1, pp.21–39.

[8] Ning, D., Wang, R., Zou, Q., Teng, B. (2016). An experimental investigation of hydrodynamics of a fixed OWC wave energy converter, Applied Energy, vol.168, pp.636–648.

[9] Setoguchi, T., Santhakumar, S., Maeda, H., Takao, M., Kaneko, K. (2001). A review of impulse turbines for wave energy conversion, Renewable Energy, vol.23, pp.261–292.

[10] Setoguchi, T., Takao, M. (2006). Current status of self rectifying air turbines for wave energy conversion, Energy Conversion and Management, vol.47, pp.2382–2396.

[11] Takao, M., Setoguchi, T. (2012). Air turbines for wave energy conversion, International Journal of Rotating Machinery, vol.2012, Article ID 717398.

[12] Takahashi, S., Nakada, H., Ohneda, H. (1992). Wave power conversion by a prototype wave power extracting caisson in Sakata port, Coastal Engineering, pp.3440–3453.

[13] Goda, Y., Suzuki, Y. (1976). Estimation of incident and reflected waves in random wave experiments, Coastal Engineering, pp.828–845.

[14] Koirala, P., Nagata, S., Imai, Y., Murakami, T. (2015). A numerical study on multi-chamber oscillating water columns, Journal of Japan Society of Civil Engineers, vol.3, no.1, pp.93–104.

[15] Okuhara, S., Takao, M., Takami, A., Setoguchi, T. (2013). Wells turbine for wave energy conversion, Open Journal of Fluid Dynamics, vol.3, DOI:10.4236/ojfd.201332A006.